ELSEVIER

Contents lists available at ScienceDirect

Brain Research Bulletin

journal homepage: www.elsevier.com/locate/brainresbull



Research report

Silencing CD28 attenuated chest blast exposure-induced traumatic brain injury through the PI3K/AKT/NF-κB signaling pathway in male mice

Zhonghua Luo^a, Changci Tong^a, Peifang Cong^a, Shun Mao^a, Ying Xu^{b,*}, Mingxiao Hou^{c,*}, Yunen Liu^{a,*}

- a Shenyang Medical College, No. 146, Huanghe North Street, Shenyang 110034, China
- b Department of Tumor Radiotherapy, the General Hospital of Northern Theater Command, No. 83 Road, Shenhe District, Shenyang 110016, China
- ^c The Second Affiliated Hospital of Shenyang Medical College, The Veterans General Hospital of Liaoning Province, No. 20 Beijiu Road, Heping District, Shenyang 110001, China

ARTICLE INFO

Keywords: Blast-induced traumatic brain injury CD28 Blood-brain barrier Inflammation PI3K/AKT/NF-kB signaling pathway

ABSTRACT

In modern war or daily life, blast-induced traumatic brain injury (bTBI) is a growing health concern. Our previous studies demonstrated that inflammation was one of the main features of bTBI, and CD28-activated T cells play a central role in inflammation. However, the mechanism of CD28 in bTBI remains to be elucidated. In this study, traumatic brain injury model induced by chest blast exposure in male mice was established, and the mechanism of CD28 in bTBI was studied by elisa, immunofluorescence staining, flow cytometry analysis and western blot. After exposure to chest shock wave, the inflammatory factors IL-4, IL-6 and HMGB1 in serum were increased, and CD3 $^+$ T cells, CD4 $^+$ and CD8 $^+$ T cell subsets in the lung were activated. In addition, chest blast exposure resulted in impaired spatial learning and memory ability, disruption of the blood-brain barrier (BBB), and the expression of Tau, p-tau, S100 β and choline acetyltransferase were increased. The results indicated that genetic knockdown of CD28 could inhibit inflammatory cell infiltration, as well as the activation of CD3 $^+$ T cells, CD4 $^+$ and CD8 $^+$ T cell subsets in the lung, improve spatial learning and memory ability, and ameliorate BBB disruption and hippocampal neuron damage. Moreover, genetic knockdown of CD28 could reduce the expression of p-P13K, p-AKT and NF- κ B. In conclusion, chest blast exposure could lead to bTBI, and attenuate bTBI via the P13K/AKT/NF- κ B signaling pathway in male mice. This study provides new targets for the prevention and treatment of veterans with bTBI.

1. Introduction

In recent years, the increased numbers of local conflicts and terrorist attacks throughout the world have increased the incidence of explosion events year by year. The blast induced-traumatic brain injury (bTBI) is a leading cause of morbidity and mortality worldwide (Marsh, Bentil, 2021). The report shows that bTBI accounts for about 30 % of all injury-related deaths, which constitutes a serious public health burden (Robinson., 2021). The types of bTBI damage include TNT, compressed air or shock tube and micro spherical explosive (Ma et al., 2014; Rubovitch et al., 2011; Beamer et al., 2016; Heldt et al., 2014; Liu et al., 2015). TNT can refer to trinitrotoluene, which is an explosive that is widely used in both military and civilian applications. In the past two decades, at least 417503 U.S. soldiers have suffered bTBI during military missions (Evans et al., 2021). Most of the wounded have no obvious

brain dysfunction in the short term, and these servicemen suffering from bTBI often return to work in advance. However, many potentially hidden neuropathological processes, including microvascular injury, axon injury and neuroinflammation, may occur within a few weeks after bTBI and have long-term adverse effects on physical, cognitive and emotional health (Raza et al., 2021). Therefore, it is more important to find some reliable biomarkers to reveal the details of the pathogenesis of bTBI.

T cell activation plays a central role in the inflammatory response, and at least two signals are required for T cells to be fully activated (Zumerle et al., 2017). The first signal is the antigen peptide-MHC molecule complex on the antigen-presenting cell which binds specifically to the T cell receptor (Janakiram et al., 2017). The second signal, a costimulatory signal, is provided by the interaction between costimulatory molecules expressed on the membranes of antigen-presenting cells and T cells, and one of the most important

E-mail addresses: 514705167@qq.com (Y. Xu), houmingxiao188@163.com (M. Hou), liuye990116@163.com (Y. Liu).

^{*} Corresponding authors.

costimulatory molecules expressed by T cells is CD28, which interacts with CD80/CD86 expressed on the membrane of antigen-presenting cells (Langenhorst et al., 2017). Moreover, cytokines promoted the activation of T cells, such as IL-2, IL-6 and IL-1 (Ptackova et al., 2018). As CD28 is a potent T cell costimulator, the inhibition of CD28 will effectively attenuate the activation of T cell (Langenhorst et al., 2018). The central nervous system inflammation and peripheral immune systems jointly regulated the process of brain damage and remodeling. Blocking the CD28/CD80 pathway can reverse the immune system imbalance and regulated inflammation to alleviate long-term brain injury in mice with cerebral ischemia (Ma et al., 2016). Selective blockade of CD28 can reduce the activation of T cells and B cells in a rhesus monkey autoimmune encephalomyelitis model, and reduce central nervous system inflammation, and prevent the pathological changes to central nervous system cells (Haanstra et al., 2015). However, the mechanism of CD28 knockout (KO) on bTBI indirectly caused by chest exposure to blast waves is still unclear.

Although it has been determined that bTBI can cause neurodegenerative diseases, the mechanism remains to be elucidated. Revealing the potential molecular mechanism of bTBI is very beneficial to interfere with and block the neurodegeneration after bTBI. There are three prominent hypotheses about bTBI, among which the chest conduction hypothesis is the most concerned (Dixon, 2017). Its core view is that the pressure shock wave acting on the chest will lead to the surge of peripheral blood volume and the increase of intracranial blood pressure, thus damaging the blood-brain barrier (BBB) and capillaries in the brain (Cernak, 2010). Another view is that primary bTBI may be a pressure wave transmitted from the chest to the brain through soft tissue or vascular system (Konan et al., 2019). The BBB is the most rigorous and solid barrier in the human body, which effectively prevents other exogenous substances from entering the brain and maintains brain function. The bTBI-related BBB damage can lead to cerebrovascular damage, including hemorrhage, hematoma, vasospasm and brain edema (Logsdon et al., 2018).

Moreover, the destruction of the integrity of the BBB will also lead to the influx of harmful substances around the body, such as unwanted cellular or microbial pathogens, which can lead to chronic inflammation and immune response. Researches have shown that repeated shock wave exposure is associated with an increase in desmin and CD13 positive pericytes and neuroinflammation, while BBB loses complete foot coverage at the end of astrocytes after exposure to bTBI (Uzunalli et al., 2021). In addition, our previous research has shown that chest shock-induced bTBI involves many important biological processes and signaling pathway changes, such as inflammation, cell adhesion, phagocytosis, neuronal and synaptic damage, oxidative stress and apoptosis (Tong et al., 2021). Therefore, we hypothesized that bTBI caused by chest blast may cause peripheral inflammatory cells to enter the brain by destroying the BBB, leading to brain dysfunction and immune inflammation by activating inflammatory pathways, which need to be further clarified.

Therefore, CD28 KO mice were selected to construct the bTBI model induced by shock wave in the chest, and the effects of silencing CD28 on the BBB, as well as T cell accumulation and activation were evaluated in this study. To explore the possible mechanism of CD28 silencing in alleviating bTBI. Our data suggest that CD28 KO can attenuate bTBI through the PI3K/AKT/NF-κB signaling pathways. These results provide new targets for prevention and treatment of veterans suffering from bTBI.

2. Materials and methods

2.1. Animals and experimental group

One hundred healthy male C57BL/6 mice, weighing 21–24 g and aged 6–8 weeks, were purchased from Beijing Vital River Laboratory Animal Technology Co., LTD., China. One hundred healthy male CD28

KO mice, weighing 21-24 g and aged 6-8 weeks, were purchased from the Jackson Laboratory (Sacramento, CA). The mice were housed 5 to a cage with adlibitum access to chow and water, under temperaturecontrolled conditions on a 12 h light/dark cycle. The C57BL/6 and CD28 KO mice were randomly assigned to the control group (n=20) and different experimental groups (12 h, 24 h, 48 h and 1 w blast), the number of mice in each experimental group is 20. In each group of mice, 5 mice organs were used in Evans blue test, 5 mice organs were tested by glucan test, 5 mice organs were detected by flow cytometry, and 5 mice organs were tested by protein immunoblotting and pathology. All animal experiments were carried out according to the National Institutes of Health Guide for the Care and Use of Laboratory Animals and approved by the Institutional Animal Care and Use Committee (Shenyang Medical College) and in compliance with the ARRIVE guidelines. All this experimental steps were in conformity to the guideline of experimental animal care and use of Shenyang Medical College, SYYXY2021092201.

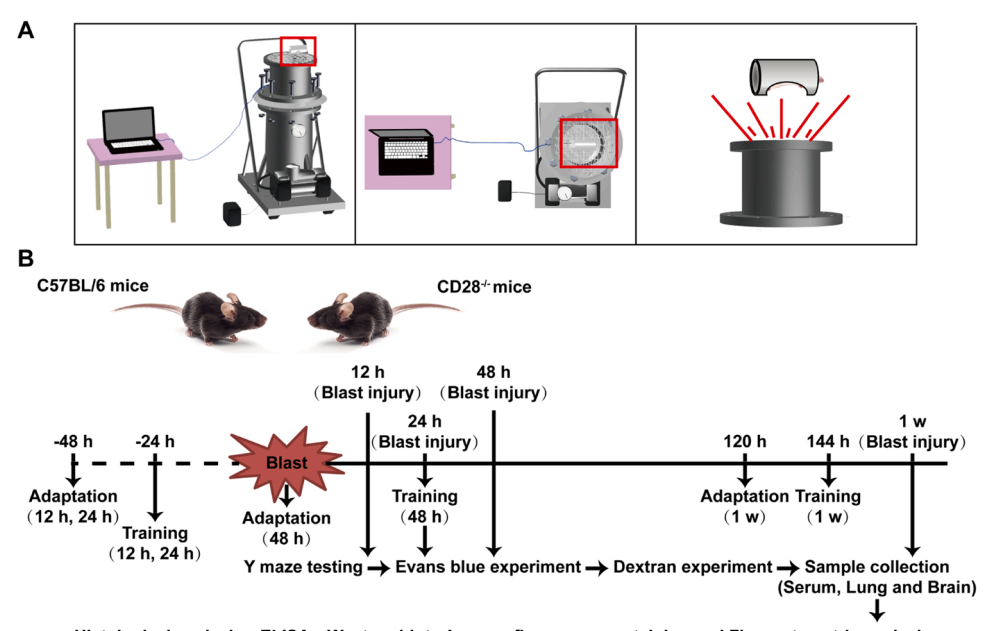
2.2. Blast exposure induced brain injury in male mice

The bTBI model was used as previously described (Tong et al., 2018). Chest explosion in this study was a mild injury. Briefly, the male mice were anesthetized by the abdominal injection of 2 % pentobarbital sodium (1.5 mL/kg; No.57-33-0; Shanghai Rongbai Biological Technology Company, China) to reduce the fear of mice in the process of model preparation. Moreover, to alleviate post-operative pain, analgesia in the form of buprenorphine (0.2 mg/kg; No. 117299, Alstoe Animal Health, UK) was administered intramuscularly prior to recovery and killing of animals. Buprenorphine was given to male mice once on the day of model preparation and the day of execution for two days. The anesthetized male mice were placed in a protective cover with their chest exposed, and aluminum foils were placed in the middle layer. After fixing the screws, the male mice were placed on the wire mesh atop the device. A pressure pump was used to increase the air pressure in the lower part of till the burst of the aluminum foils. The compressed air rapidly expanded from the blasting port at high speed, forming blast waves that impacted the chest of male mice. The pressure detected by a pressure sensor was transmitted through a data cable and recorded by a computer. The overpressure value of the shock wave at the instant of blasting was 115.8 \pm 10.4 per square inch (PSI). The male mice model and experimental timeline were shown as Fig. 1.

2.3. Y maze in male mice

The animals' body weight was reduced to 80 percent of that of normal male mice by fasting two days earlier. Adaptation period: one day of adaptation was carried out in the first 2 days of different experimental time points (12 h, 24 h, 48 h and 1 w). The male mice were placed in the Y maze palace for about 10 min each time. It could adapt three times a day without food. Training period: 120 h for adaptation training and 144 h for formal training. Training was carried out one day before different experimental time points. The food was placed into one arm of the Y maze, and the food was bait. The other arm of the door was closed, and place the mice over the starting arm so that the mice could find the food, and guide if necessary. Each training lasts for 10 min, 3 times a day. Test period: the test was carried out at 12 h, 24 h, 48 h and 1 w after the success of the model. The software was opened, then the doors of the three arms of the Y maze were simultaneously opened, the fasting male mice were placed in the starting arm, and the number of times the mice entered each arm and the stay time were recorded within 5 min.

The three arms and the central region of Y maze were set as four regions respectively using the animal motion trajectory tracking system (Model: ethovision XT, Netherlands: Noldus). The position of male mice was located by the camera, the time that the mice stayed in a certain area and the number of times they entered the area were recorded by the



Histological analysis, ELISA, Western blot, Immunofluorescence staining and Flow cytometric analysis

Fig. 1. Model sketch and experimental timeline. (A) The simulation device for explosive injury and the schematic diagram of the model preparation. (B) The experimental timeline. After exposure of chest to blast waves leading to ALI in C57BL/6 mice and CD28^{-/-} mice, serum, lung and brain tissue samples were taken at 12 h, 24 h, 48 h and 1 w for subsequent detection.

animal motion trajectory tracking system.

2.4. Evans blue experiment in male mice

The five C57BL/6 male mice and five CD28 KO male mice in each group were used in the Evans blue experiment. After lung injury evaluation, Evans blue (No. E8010, Solarbio, China) was used to evaluate BBB permeability. The male mice were intraperitoneally anesthetized with 2 % sodium pentobarbital (1.5 mL/kg) to reduce the fear of mice in the process of model preparation. Evans blue was injected into the vein 30 min before perfusion, and then 0.9 % of the saline was perfused for 15 min. Local anesthesia was performed on the thoracic cavity 3 min before dissection in the form of subcutaneous bupivacaine (No. 02848/ 0198, Mercury Pharma, UK). The brain was photographed and weighed. The brain tissues were homogenized in 0.5 mL 50 % trichloroacetic acid (No. T8100, Solarbio, China). The samples were incubated for 24 h at 37 $^{\circ}\text{C}\text{,}$ and centrifuged at 12,000 rpm for 10 min at 4°C. Next, the supernatant was sucked up. The OD (absorbance) value of the samples was determined by iMarkTM Microplate Reader (Bio-Rad Laboratories, USA). The standard curve was established using the OD value of Evans blue gradient concentration, and the content of EB in the brain tissue exudates was calculated.

2.5. Dextran experiment in male mice

The five C57BL/6 male mice and five CD28 KO male mice in each group were used in the dextran experiment. The fluorescein isothiocyanate-dextran 40 kD (FITC-dextran 40 kD, 500 mg/kg, No. FD40, Sigma-Aldrich, USA) was used to evaluate BBB breakdown. Briefly, 12 h, 24 h, 48 h and 1 w after lung injury, FITC-dextran was given intravenously to mice over 2 h. The male mice were then perfused transcardiacally, and the brains were removed and fixed in 4 % paraformaldehyde in PBS at 4 $^{\circ}$ C for 24 h. The fixed-brain tissues were then sliced into 20- μ m-thick coronal sections with a freezing microtome. Finally, the samples were observed and photographed with a fluorescence microscope.

2.6. Sample collection and processing in male mice

At 12 h, 24 h, 48 h and 1 w after blast exposure, the lung and brain tissues were collected. Briefly, after 12 h of fasting and 4 h of water deprivation preoperatively, the male mice were intraperitoneally anesthetized with 2 % sodium pentobarbital (1.5 mL/kg, No. 57-33-0, Shanghai Rongbai Biological Technology Company, China) and fixed on the operating table in a prone position. The abdominal cavity was opened, and the blood was harvested through the abdominal aorta to be sacrificed. The cranial cavity and pleural were opened, and the lung and brain tissues of all male mice were taken. The whole blood of male mice was placed in the collecting vessel for 30 min, 3000 rpm, centrifuged for 10 min, and the serum was taken and stored in a refrigerator of -80° C. The ratio of wet to dry weight of one third of the brain tissue was calculated, and the direction of change was opposite to the direction of edema formation. Part of the lung and brain tissues in every group were immersed in 10 % formalin buffer (No.G2161, Solarbio, China) for pathological examination, while part of the lung and brain tissues in every group were placed in a nitrogen canister for protein determination.

2.7. Enzyme linked immunosorbent assay (ELISA) in male mice

The serum IL-4 (SEA077Mu, Cloud-Clone Company, USA), IL-6 (SEA079Mu, Cloud-Clone Company, USA), and HMGB1 (SEA399Mu, Cloud-Clone Company, USA) levels were measured using an elisa kit as per manufacturer's instructions. The experimental procedures were carried out in accordance with the instructions of the reagents. Optical density values were measured at 450 nm with a microplate reader (imark, Bio-Rad, USA). The standard curves were used to calculate concentrations in each sample.

2.8. Histological analysis in male mice

The brain and lung tissues for histological analysis were fixed in 10 % formaldehyde (No. G2161, Solarbio, China) at room temperature and embedded in paraffin blocks using a Leica Microsystem tissue processor (ASP 300 S, Germany). For histological staining, Leica

Microsystem microtome (Model RM 2265, Germany) was used for slicing, and the thickness of slicing was 3–5 μm , which were stained with hematoxylin and eosin (H&E). Lung injury score: Score 0, normal lung tissue without inflammation, edema, or bleeding. 1 point, mild lung injury, a small amount of inflammatory cell infiltration and edema around the alveoli, but no obvious bleeding. 2 points, moderate lung injury, marked infiltration of inflammatory cells around the alveoli, edema, and minor bleeding. 3 points, severe lung injury, a large number of inflammatory cell infiltration and edema around the alveoli, accompanied by obvious bleeding necrosis. Brain injury score: 0 score, no inflammation around blood vessels. 1 point, There is a small amount of inflammatory cell infiltration around the blood vessels. 2 points: there is obvious inflammatory cell infiltration around the blood vessels. 3 points, there is a large number of inflammatory cell infiltration and edema around the blood vessels.

2.9. Immunofluorescence staining in male mice

The expression and localization of brain injury protein S100ß and pathway proteins NF-κB, p-PI3K and p-AKT in the C57BL/6 mice and CD28 genetic knockout male mice were determined in the control group and different experimental groups (12 h, 24 h, 48 h and 1 week). The brain tissues were dewaxed with xylene, hydrated with a graded alcohol series, incubated with 3 % H_2O_2 (80 % methanol) for 30 min, and washed 3 times with PBS for 5 min. Antigen was repaired by the highpressure thermal antigen repair method. The samples were blocked with 10 % goat serum (No. SL038, Solarbio, China) for 30 min and incubated with primary antibody (Tab.S1) overnight at 4°C in a wet box, and stained with a fluorescent secondary antibody goat anti-mouse IgG H&L Alexa Fluor® 647 (1:200, No. ab150115, Abcam, UK, RRID: AB_2687948) and goat anti-rabbit IgG H&L Alexa Fluor® 488 (1:200, No. ab150077, Abcam, UK, RRID: AB_2630356) after washing 3 times with PBS for 5 min. Finally, the samples were observed and photographed with a fluorescence microscope (PA53 FS6).

2.10. Flow cytometric analysis in male mice

The recruitment and subtypes of T cells in the lung and brain tissues of the control group (the C57BL/6 male mice and the CD28 genetic knockout male mice) and blast injury groups (12 h, 24 h and 48 h in the C57BL/6 male mice, 24 h in the CD28 genetic knockout male mice) were detected. The cells were isolated from the lung and brain tissues. The individual lung and brain tissue were excised, cut into small pieces, and enzymatically digested in 5 mL of collagenase digestion buffer (HBSS without Ca+/Mg+) (No. C8140, Solarbio, China), 1.5 mg/mL collagenase type I (No. C8140, Solarbio, China) at 37°C for 30 min with agitating, then subsequently transferred into 5 mL of collagenase/dispase digestion buffer (HBSS without Ca+/Mg+, 1 mg/mL collagenase/ dispase (No. C8140, Solarbio, China) for another 20 min at 37°C with agitating, and pressed against the bottom of a 100 µm strainer with the plunger of a 3 mL syringe. The single cells from tissues were washed through the strainer with 10 mL cold buffer (PBS+0.5 %BSA+2 mM EDTA). The red cell lysis buffers were used to perform red cell lysis (No. R7757, Sigma, USA), the cells were counted using a hemocytometer. The single cell suspensions were pre-incubated with anti-mouse CD16/32 antibody (1:100, No.553142, BD Biosciences, USA, RRID: AB 394657) to prevent nonspecific binding of antibodies to FcRy followed by multistaining with fluorescence directly conjugated primary antibodies (Tab. S2). The dead cells were stained with propidium iodide staining solution. The samples were subjected to FACS Aria II analysis (BD Biosciences). The data were analyzed by FlowJo_V10 (FlowJo, OR) software. Detection of the percentage and numbers of activation and accumulation of CD3+ T cells, CD4+ and CD8+ subsets of T cells was executed by immunofluorescence analyses using the antibodies conjugated to allophycocyanin (APC), peridinin chlorophyll proteincyanine5.5 (PerCP-Cy5.5), fluorescein isothiocyanate (FITC), peridinin

chlorophyll protein (PerCP), allophycocyanin/cyanine7 (APC/Cy7) and phycoerythrin-cyanine7 (PE-Cy7). The minimum of 50,000 lymphocytes was obtained for each antibody assortment. Activation and accumulation of CD3+ T cells, CD4+ and CD8+ subsets of T cells were demarcated by the positivity of CD3, CD44, CD4, CD8 and CD62L, respectively. The CD4 and CD8 cells were primarily gated, and then the dot plot analyses of subsets were derived from these gated CD4⁺ and CD8⁺ cell populations and reported.

2.11. Western blotting

The whole protein was extracted from the brain and lung tissues using a tissue protein extraction kit (No. FD0889, Hangzhou Fude Biological Technology Company, China), and the protein concentration was determined by a BCA protein assay kit (No. FD2001, Hangzhou Fude Biological Technology Company, China). The main components of RIPA cracking solution were 50 mM Tris (pH 7.4), 150 mM NaCl, 1 %TritonX-100, 1 % sodium deoxycholate, 0.1 % SDS. The expression of CD8, IL-4, IL-6 and HMGB1 in lung tissues of C57BL/6 mice and CD28 KO mice were detected in control group and different experimental groups (12 h, 24 h, 48 h, 1 w). The brain tissues CD8, brain damage proteins Tau, p-Tau, S1008, choline acetyltransferase were detected. The expressions of CD8, brain injury protein Tau, p-Tau, S100\beta and choline acetyltransferase in brain tissues were detected. The expression of inflammation-related proteins IL-1 β , IL-4, IL-10 and TNF- α were determined. The pathway proteins NF-κB, PI3K, p-PI3K, AKT and p-AKT were also determined. The protein samples were added with a corresponding proportion of loading buffer, boiled and denatured for 5 min. Next, the samples were subjected to 10 % SDS-PAGE electrophoresis, then were transferred to 5 % skim milk PBST buffer at room temperature for 1 h, and washed with PBST 3 times. Next, the appropriate primary antibody (Tab.S3) were added and incubated overnight at 4°C. The membrane was washed 3 times with PBST, and a horseradish peroxidase-labeled goat anti-mouse secondary antibody (1:4000, No. ab6789, Abcam, UK, RRID: AB_955439), goat anti-rabbit secondary antibody (1:4000, No. ab6721, Abcam, UK, RRID: AB_955447) and goat anti-rat secondary antibody (1:2000, No. ab7097, Abcam, UK, RRID: AB_955411) were incubated for 1.5 h at room temperature, respectively. The film was washed 3 times. The film were visualized using a ClarityTM Western ECL Substrate (No.170-5061, Bio-Rad Laboratories, USA) and a Tanon 5200 chemiluminescence image analysis system (Tanon Science and Technology Co., Ltd., Shanghai, China).

2.12. Statistical analysis

The SPSS 21.0 software was used for statistical analysis and the data were expressed as "mean \pm standard deviation". One-way analysis of variance was used for comparison between groups (ANOVA). The significance was determined when p values < 0.05. The data were analyzed and plotted using GraphPad Prism 8.0.

3. Results

3.1. CD28 KO ameliorates the expression of serum inflammatory factors and lung injury

CD28 KO can improve the expression of serum inflammatory factors and lung injury, as shown in Fig. 2. Compared with the control group, the serum levels of IL-4, IL-6 and HMGB1 in the blast injury group were significantly increased (p< 0.05), peaked at 12 h, and then gradually decreased (Fig. 2A–C). However, CD28 KO significantly inhibited the increase of serum levels of IL-4, IL-6 and HMGB1 (Fig. 2A–C). As shown in Fig. 2D, compared with the control group, the expression of CD28 in the lung tissues was significantly increased in the blast injury group (p< 0.05). As shown in Fig. 2F, the expression of CD28 in the lung of CD28 KO male mice was significantly down-regulated, indicating that CD28

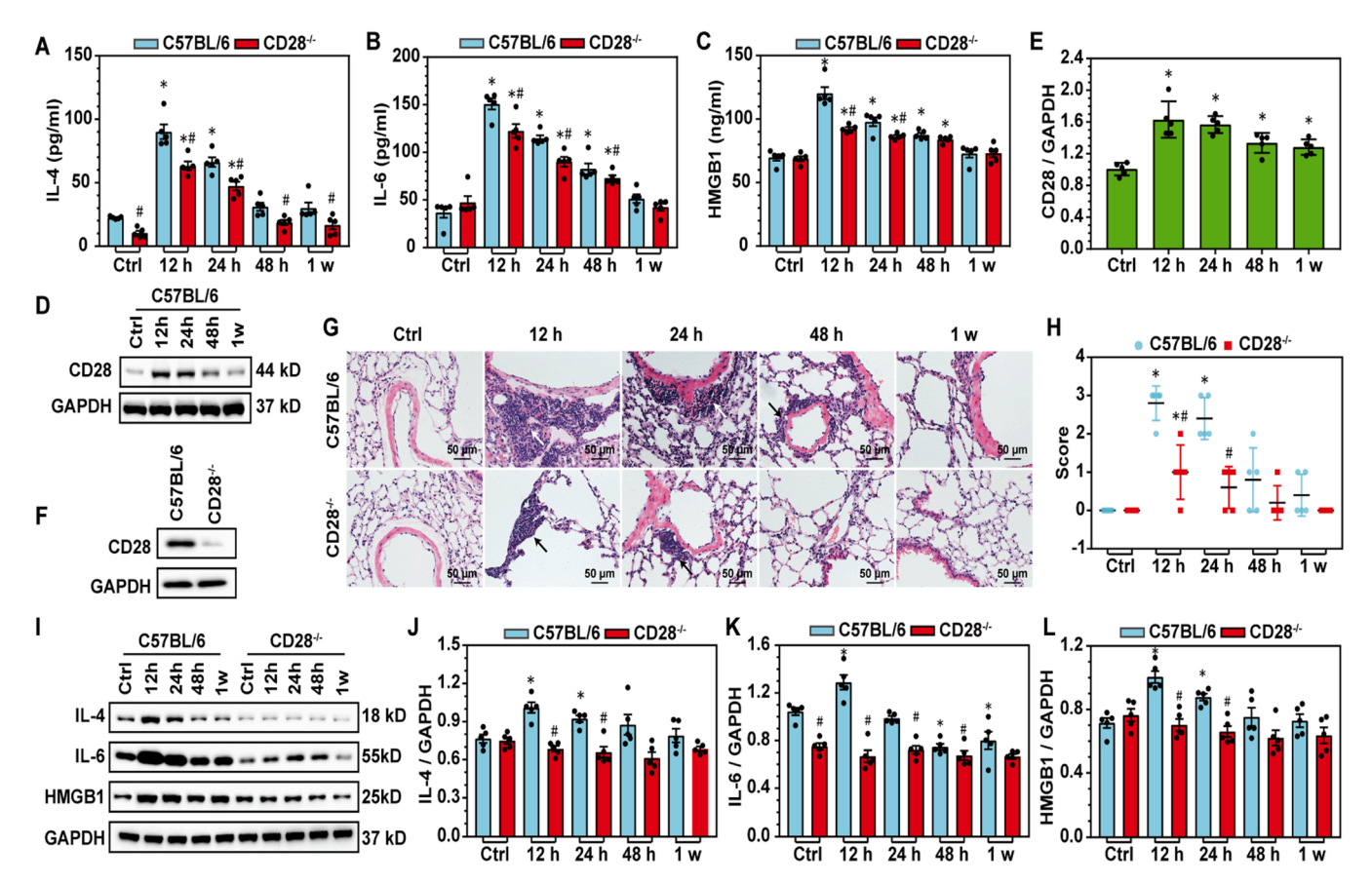


Fig. 2. CD28 KO ameliorates the increased serum inflammatory factors and lung inflammation. (A-C) ELISA was used to detect serum inflammatory factors IL-4, IL-6 and HMGB1. (D-E) The protein level (CD28) were normalized to GAPDH, Fig. 2E is the OD number of 2D. GAPDH was used as a reference. (F) CD28 protein knockout effect in the lung tissues of CD28. male mice. (G) HE staining was used to detect pathological changes in the lung tissues of C57BL/6 male mice and CD28. male mice after blast exposure at different times. (H) Pulmonary inflammation score was analyzed. (I-L) Western blot analysis was used to detect the expression of IL-4, IL-6, and HMGB1 in the lung tissues after blast exposure of C57BL/6 male mice and CD28-/- male mice at different times. GAPDH was used as a reference. Results were expressed as the mean \pm S.D (n = 5 per group). *p < 0.05 versus the control group; *p < 0.05 versus the C57BL/6 group ((two-way ANOVA, Bonferroni post hoc test). CD28. CD28. CD28 knockout mice.

was effectively silenced in CD28 KO male mice. Compared with the control group, the inflammation score in the lung tissues peaked at 12 h and then gradually decreased, whereas CD28 KO significantly improved the inflammation score after shock wave exposure (Fig. 2G–H). As shown by western blot, the expression of IL-4, IL-6 and HMGB1 was increased after blast exposure, and CD28 KO improved the expression of serum inflammatory factors and the lung injury after blast exposure.

3.2. CD28 KO inhibited the activation and accumulation of CD3 $^+$ T cells, CD4 $^+$ and CD8 $^+$ subsets of T cells in the lungs

To determine the effect of CD28 on T cell activation, the percentage and number of CD3 $^+$ T cells and activated CD3 $^+$ T cells in the lung tissues by flow cytometry were analyzed, the results were shown in Fig. 3. When the C57BL/6 male mice were exposed to shock waves, the percentage and number of CD3 $^+$ T cells and activated CD3 $^+$ T cells in the lung tissues were increased, reached its peak at 12 h, and then gradually decreased over time (Fig. 3A). The CD28 KO effectively inhibited the percentage and number of CD3 $^+$ T cells and activated CD3 $^+$ T cells induced by blast wave exposure for 24 h (Fig. 3A–E). In the CD28 KO male mice, the maximum number of CD3 $^+$ T cells was 9.2 $^+$ 10 3 . Although blast wave exposure could induce an increase in CD3 $^+$ T cells in the lung tissues of CD28 KO male mice, it could not activate them. The percentage and total number of CD3 $^+$ T cells in C57BL/6 male mice after chest detonation were the highest at 12 h and the lowest at 48 h. Therefore, to ensure the validity of the data, the 24-h time point was

selected. From this it can be seen, blast wave exposure significantly increased the percentage and number of CD4+ and CD8+ T cells, while CD28 KO effectively inhibited the percentage and number of CD4+ and CD8+ T cells induced by blast exposure (Fig. 3F–K). CD28 KO can inhibit the activation and accumulation of CD3+ T cells induced by blast wave exposure, the effect of CD28 KO on the activation and aggregation of CD4+ and CD8+T cells was further determined.

3.3. CD28 KO alleviated spatial learning and memory impairment, BBB destruction, and brain damage

The experimental results were shown in Fig. 4. In the Y-maze experiment, the retention time and entry times of mice in the food arm were significantly reduced after blast exposure, and CD28 KO could effectively slow down the recovery of the retention time and entry times of mice in the food arm (p< 0.05). As shown in Fig. 4D, there were no significant changes in male mice brain tissues before and after the blast exposure injury. Moreover, The results in Fig. 4E demonstrated that the wet-dry weight ratio of the brain tissues was slightly higher at 24 h after blast compared with the control group, indicating that the blast induced mild brain edema, whereas the edema degree was reduced in the CD28 KO male mice. Evans blue extravasation was used to evaluate the degree of BBB damage, and the results indicated that there was obvious Evans blue extravasation in brain tissues after blast exposure. Evans Blue showed the most severe leakage at 12 h, decreased at 24 h and increased again at 48 h. According to the results in Fig. 4F–G, CD28 KO reduced

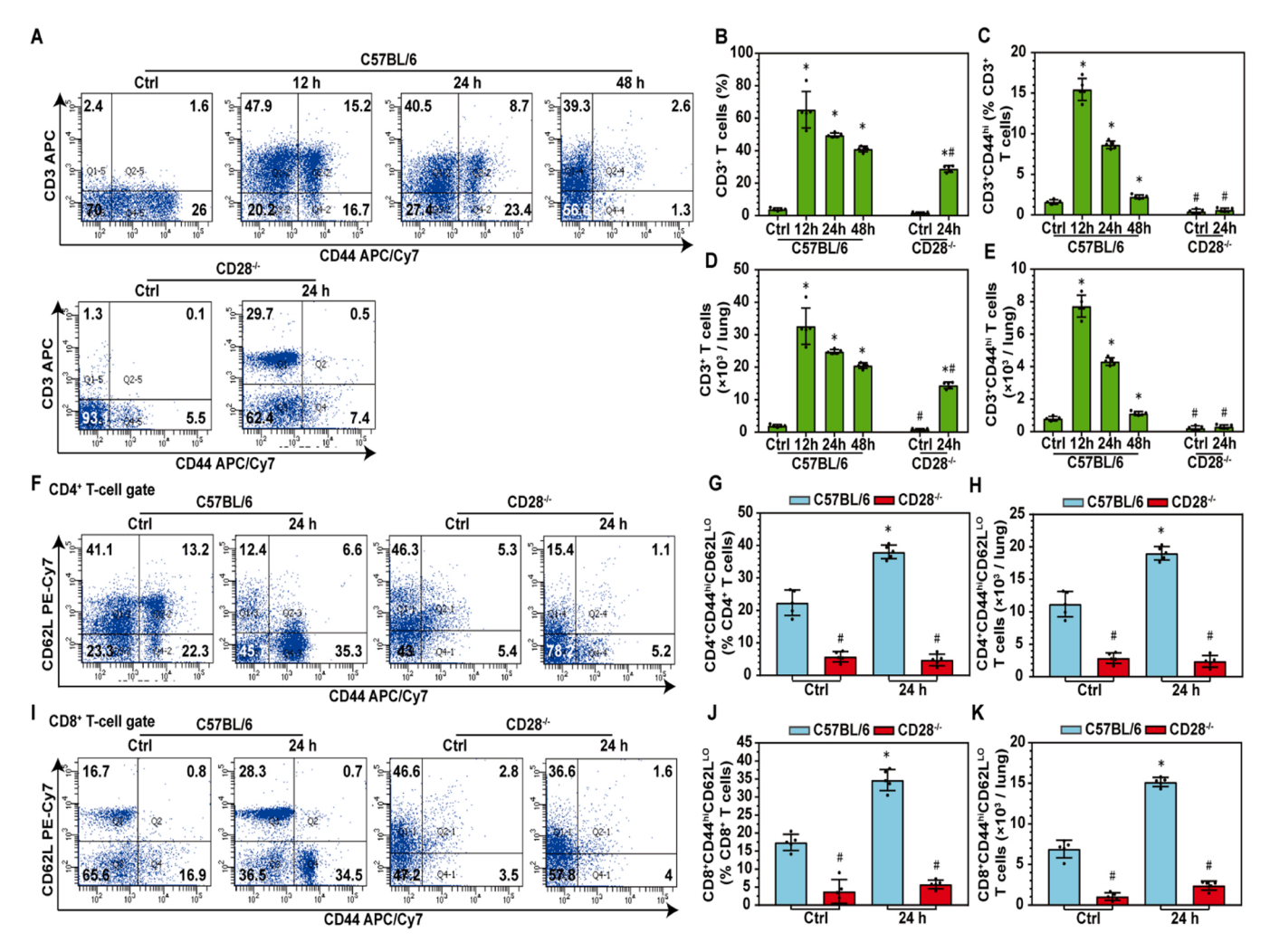


Fig. 3. CD28 KO inhibited the activation and accumulation of CD3⁺ T cells and CD4⁺ and CD8⁺ subsets of T cells in the lungs of mice exposed to blast waves. Flow cytometry data were collected from C57BL/6 male mice (Control group, 12 h, 24 h and 48 h after blast exposure) and CD28^{-/-} male mice (Control group, 24 h after blast exposure). (**A-E**) Flow cytometry plots and quantitative data represent the percentage and total numbers of CD3⁺ T cells and CD3⁺CD44^{hi} T cells (activated effector T cells) in the lung tissues. (**F-H**) Flow cytometry plots and quantitative data represent the percentage and total numbers of CD44^{hi} CD62L^{lo} T cells (effector memory T cells) within the CD4⁺ population of lungs. (**I-K**) Flow cytometry plots and quantitative data represent the percentage and total numbers of CD44^{hi} CD62L^{lo} T cells within the CD8⁺ population of lungs. Results were expressed as the mean ± S.D (n = 5 per group). *p < 0.05 versus the control group, *p < 0.05 versus the C57BL/6 group (two-way ANOVA, Bonferroni post hoc test). CD28⁻C CD28 knockout mice.

BBB damage caused by blast exposure. Dextran also exhibited the most serious leakage at 12 h, decreased at 24 h and increased again at 48 h, while CD28 KO reduced BBB damage induced by blast exposure, and dextran had no upward trend. As shown in Fig. 4J–K, compared with the blast injury groups, the degree of hippocampal neuron injury in the CD28 KO male mice was significantly decreased (p< 0.05). The CD28 KO can attenuate the hippocampal neuronal damage; after 1w, the neuronal damage in the CD28 KO male mice was observably higher compared with the control group without blat exposition, whereas the neuronal damage still lower than the control male mice exposed to the blast waves.

3.4. Effect of CD28 KO on expression of brain injury markers

The results were shown in Fig. 5. Explosion exposure resulted in increased expression of CD28 in the brain tissues, and the peak of CD28 expression in the brain tissues was 48 h, which was different from that in the lung tissues at 12 h (Fig. 5A). Compared with the control group, the expression of t-Tau, p-Tau, S100 β , and choline acetyltransferase was significantly increased in the C57BL/6 male mice (Fig. 5C). Whereas the expression of t-Tau, p-Tau, S100 β and choline acetyltransferase was

signally decreased in the CD28 KO male mice compared with the C57BL/6 male mice (Fig. 5C–G). The results of immunofluorescence indicated that S100 β expression was memorably raised after blast exposure, and the CD28 KO could effectively reduce the expression of S100 β (Fig. 5J).

3.5. CD28 KO reduced inflammatory cell infiltration and cytokines

As shown in Fig. 6A, compared with the control group, infiltration of inflammatory cells around blood vessels in the brain tissues appeared after blast exposure, and peaked at 48 h. This phenomenon was different in the lung tissues, in which inflammatory cell infiltration became most serious at 12 h, while inflammatory cell infiltration in the CD28 KO male mice was evidently reduced compared with the C57BL/6 male mice. Furthermore, blast exposure increased the expression of the IL-1 β , IL-4, and TNF- α in the brain tissues, and peaked at 48 h, which was delayed compared with the peaking time in the lung tissues (Fig. 6D,E,G). The CD28 KO observably decreased the expression of IL-1 β , IL-4, and TNF- α , and increased the expression of IL-10 compared with the C57BL/6 male mice (Fig. 6D-F).

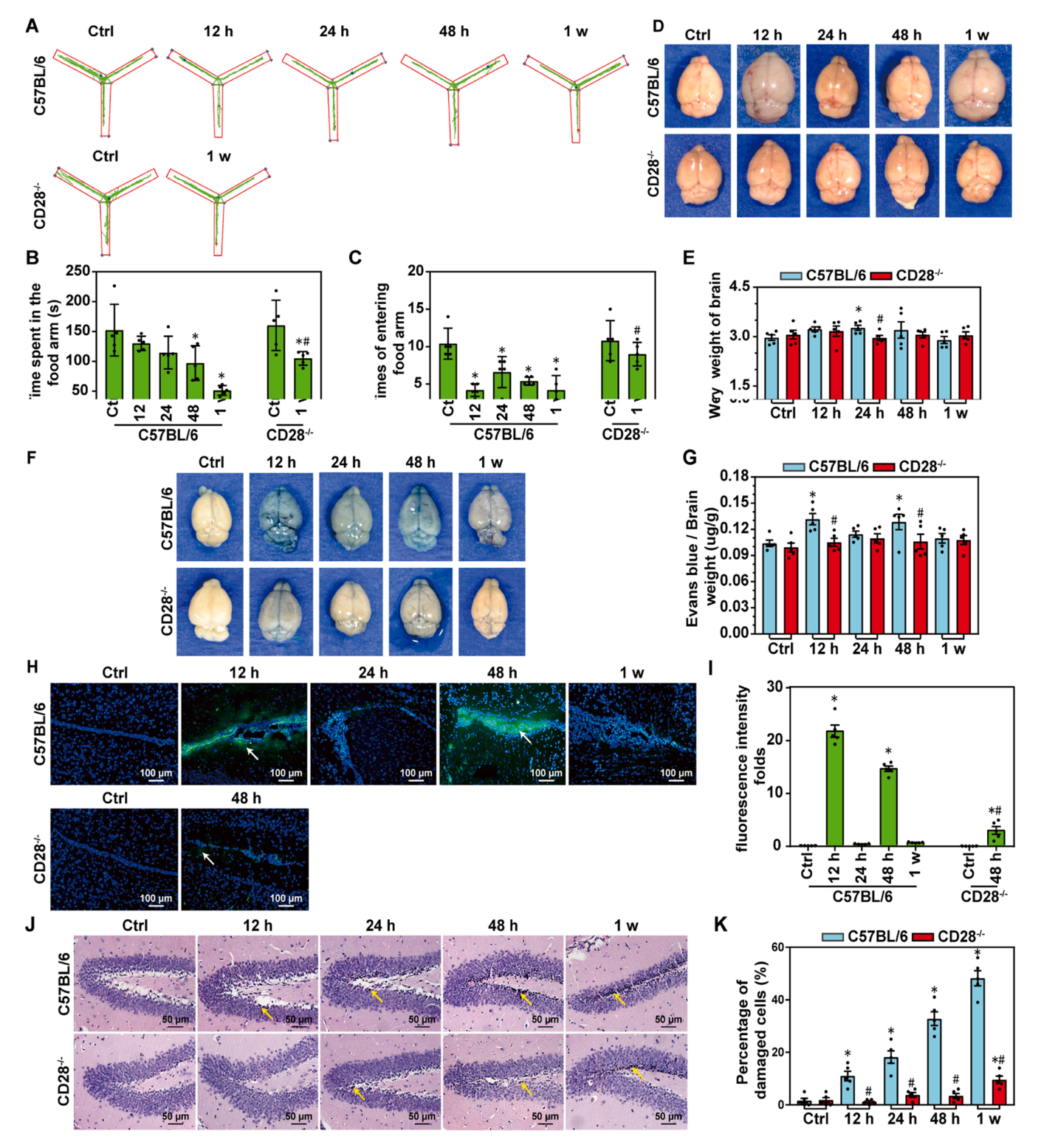


Fig. 4. CD28 KO alleviated spatial learning and memory impairment, brain edema, BBB damage and neuronal damage in the hippocampus induced by blast exposure. (A) The road map of mice in Y maze. (B) Time spent in the food arm of male mice. (C) The number of times a mouse enters the food arm. (D) General picture of the male mouse brain. (E) The ratio of wet weight to dry weight of the brain. (F) Evans blue assay was used to detect BBB and brain images. (G) Evans blue permeability analysis. (H) Representative images of FITC-dextran extravasation in the brains. (I) Fluorescence intensity of FITC dextran. (J-K) HE staining in the hippocampus and the percentage of damaged cells in the hippocampus. Results were expressed as the mean \pm S.D (n = 5 per group). *p < 0.05 versus the control group, *p < 0.05 versus the C57BL/6 group (two-way ANOVA, Bonferroni post hoc test). CD28 '/: CD28 knockout mice

3.6. CD28 KO suppressed the activation and accumulation of CD3 $^+$ T cells, CD4 $^+$, and CD8 $^+$ subsets of T cells in the brain

To determine the effect of CD28 on T cell activation, the percentage

and number of CD3⁺ T cells and activated CD3⁺ T cells in the brain tissues by flow cytometry were analyzed. The percentage and number of CD3⁺ T cells and activated CD3⁺ T cells were increased after the C57BL/6 male mice exposed to blast waves at 24 h and 48 h, and reached its

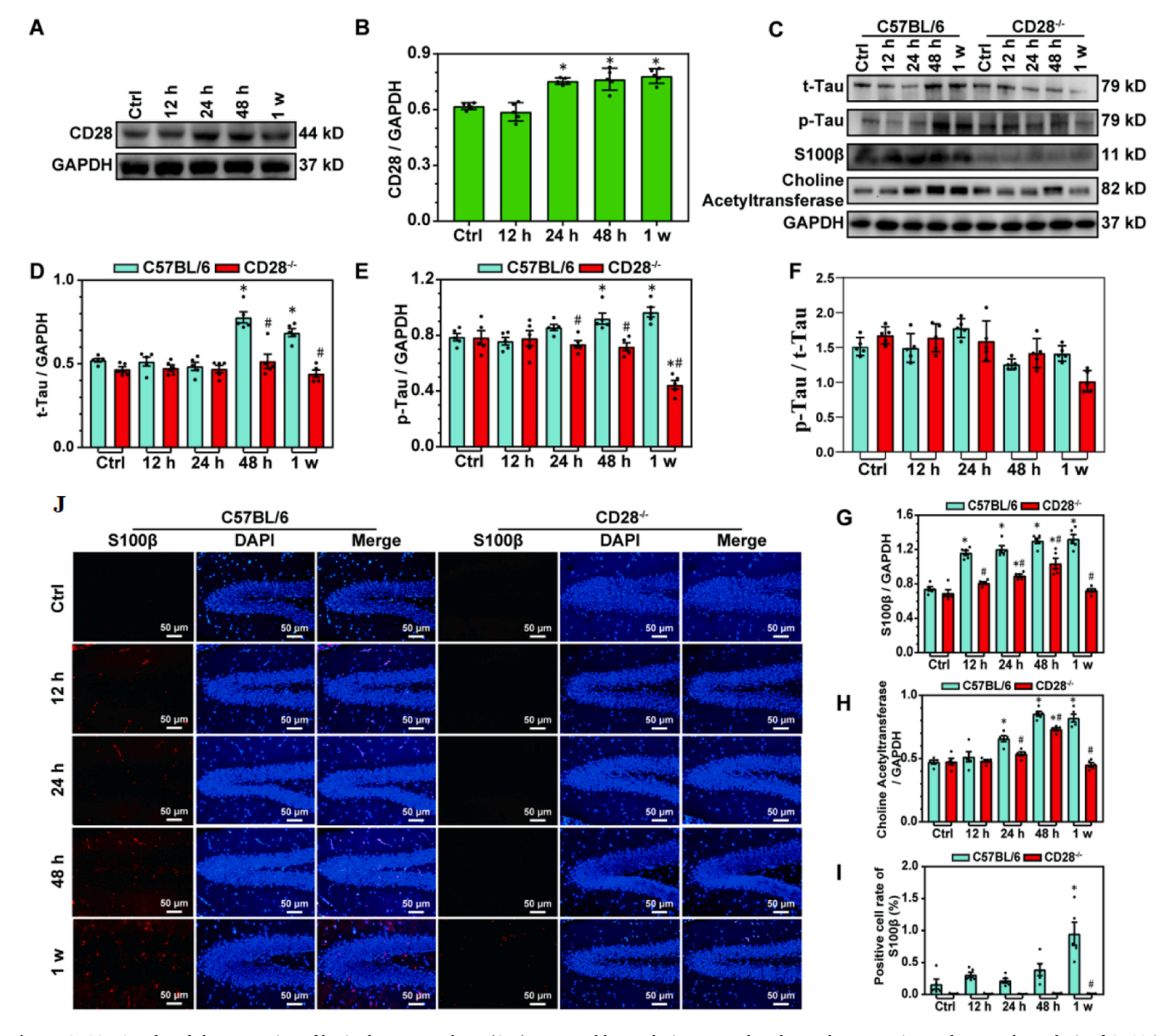


Fig. 5. CD28 KO reduced the expression of brain damage markers. (A-B) Western blot analysis was used to detect the expression and grayscale analysis of CD28 in the brain tissues tissue after blast exposure. (C-G) Western blot analysis was used to detect the expression of Tau, p-Tau, S100β and choline acetyltransferase in brain tissues. GAPDH was used as a reference. (H-I) Immunofluorescence staining of S100β (red) and DAPI (blue) was performed on the sections of C57BL/6 and CD28 KO male mice. The positive cell rate of S100β was analyzed. Results were expressed as the mean \pm S.D (n = 5 per group). *p < 0.05 versus the control group, *p < 0.05 versus the C57BL/6 group (two-way ANOVA, Bonferroni post hoc test). CD28'/: CD28 knockout mice

peak at 48 h, which was significantly delayed compared with the peak of CD3⁺ T cells in the lung tissues at 12 h (Fig. 7A–E). The CD28 KO effectively inhibited the percentage and number of CD3+ T cells and activated CD3⁺ T cells caused by blast exposure for 24 h (Fig. 7A-E). Although blast exposure could induce an increase in CD3⁺ T cells in the brain tissues of the CD28 male mice, it could not activate them. The percentage and total number of CD3+ T cells in C57BL/6 male mice after chest detonation were the highest at 48 h and the lowest at 12 h. Therefore, to ensure the validity of the data, the 24-h time point was selected. Because CD28 KO remarkably inhibited the activation and accumulation of CD3⁺ T cells induced by blast exposure, the effect of the CD28 KO on the activation and aggregation of CD4 + and CD8 + T cells was further determined. Blast exposure significantly increased the percentage and number of CD4+ and CD8+ T cells, while the CD28 KO effectively inhibited the percentage and number of CD4⁺ and CD8 T cells induced by blast exposure (Fig. 7F-K).

3.7. CD28 KO attenuated bTBI through the PI3K/AKT/NF- κB signaling pathway

As shown in Fig. 8, compared with the control group, blast exposure significantly increased the expression of p-PI3K, p-Akt and NF- κ B in the brain tissues, whereas the CD28 KO markedly inhibited the expression of p-PI3K, p-AKT and NF- κ B (Fig. 8A–F). Moreover, the immunofluorescence results also demonstrated that the expression of p-PI3K, p-AKT and NF- κ B was significantly increased after blast exposure, and the CD28 KO could effectively inhibit the expression of p-PI3K, p-AKT and NF- κ B (p < 0.05) (Fig. 8H–J).

4. Discussion

The explosion not only damages the lung tissue, but also obviously reduces the heart rate and blood pressure, increases breathing and even

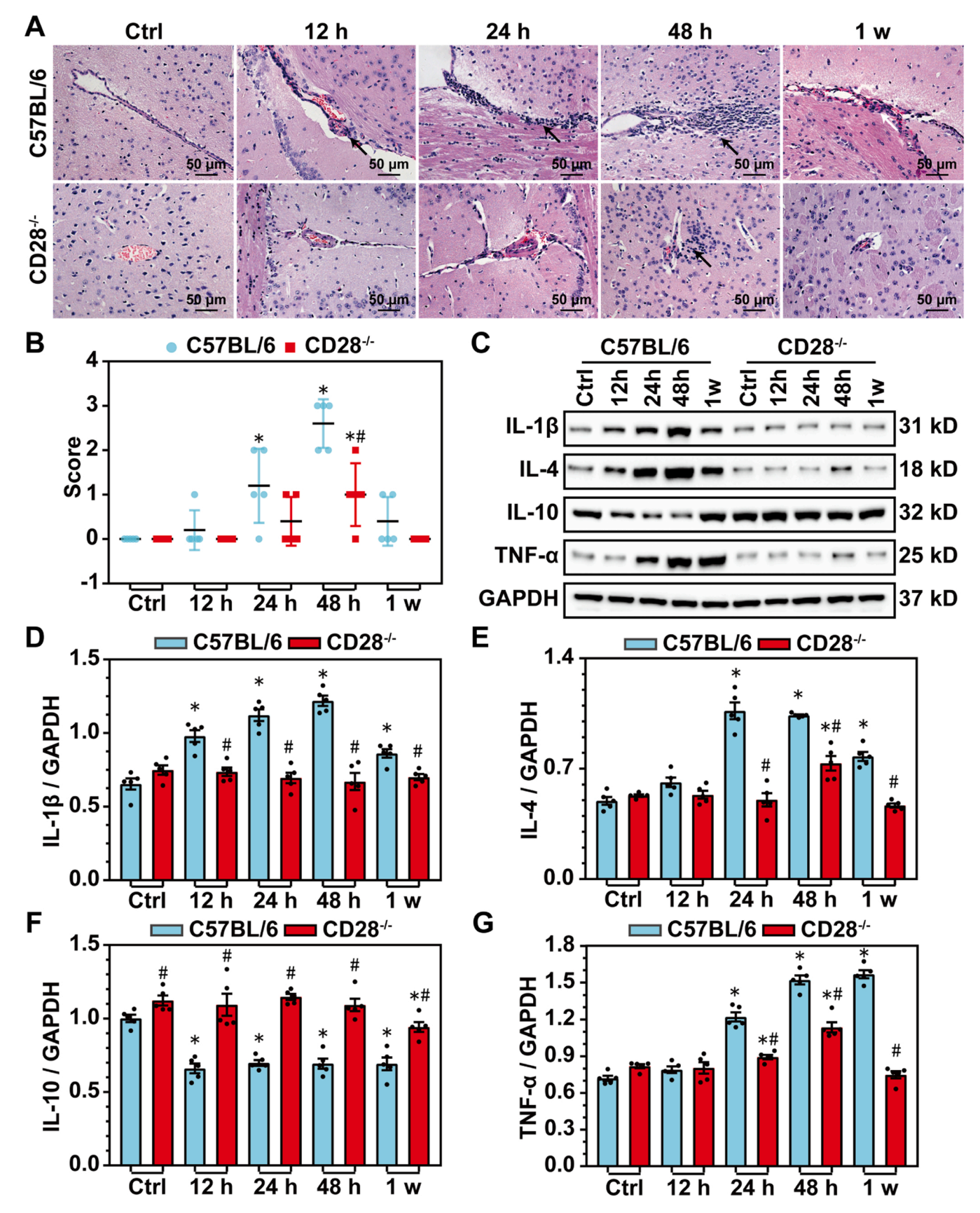


Fig. 6. CD28 KO reduced infilammatory cell infiltration and cytokines. (A) HE staining in the brain tissues. (B) The score of inflammation. (C-G) Western blot analysis was used to detect the expression of IL1β, IL-4, IL-10 and TNF-α in the brain tissues. GAPDH was used as a reference. Results were expressed as the mean \pm S.D (n = 5 per group). *p < 0.05 versus the control group, *p < 0.05 versus the control group, *p < 0.05 versus the control group, *p < 0.05 versus the C57BL/6 group (two-way ANOVA, Bonferroni post hoc test). CD28 '/: CD28 knockout mice

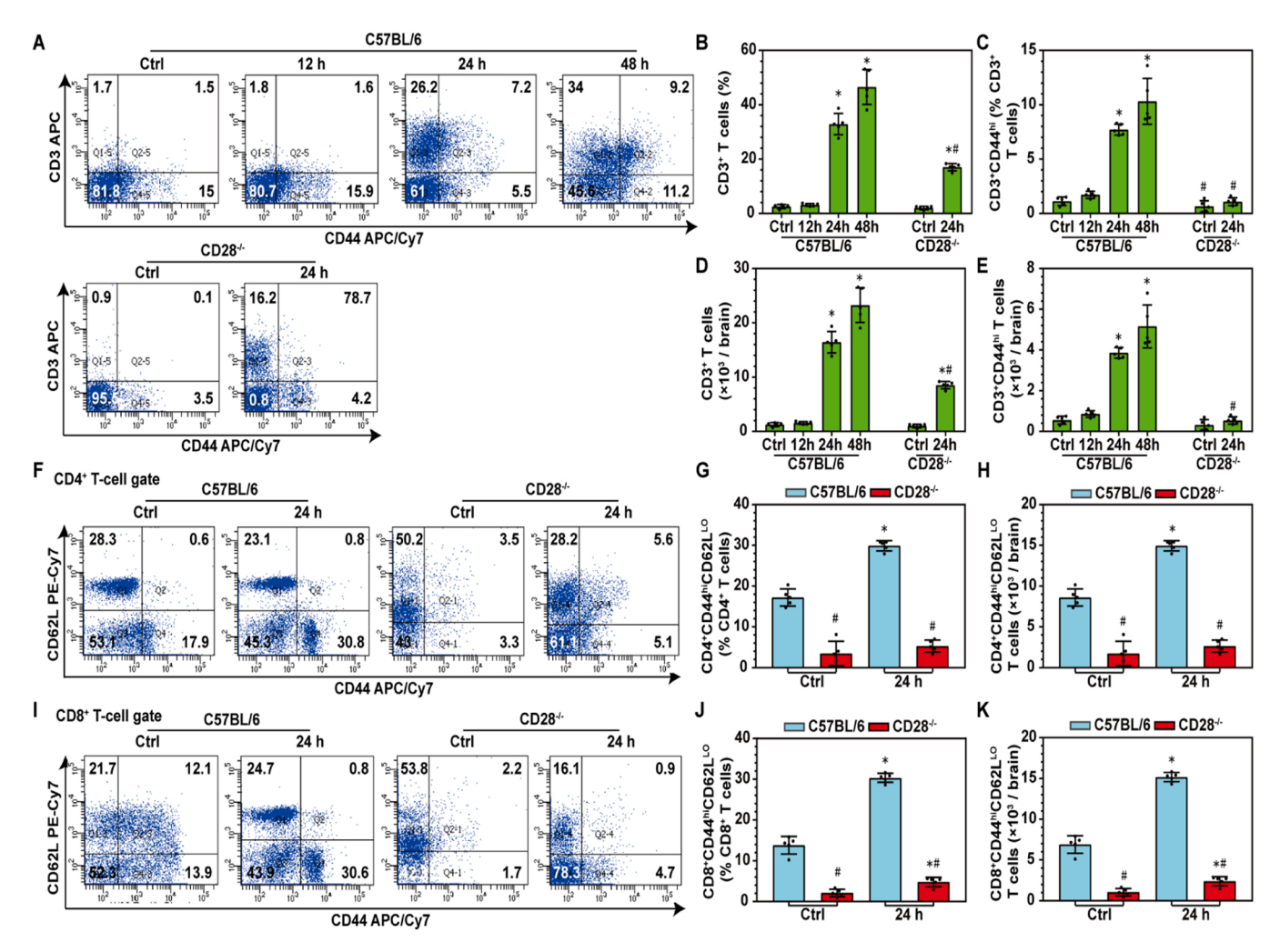


Fig. 7. CD28 KO inhibited the activation and accumulation of CD3 $^+$ T cells, CD4 $^+$, and CD8 $^+$ subsets of T cells in the brain tissues. (A-E) Flow cytometry plots and quantitative data represent the percentage and total numbers of CD3 $^+$ T cells and CD3 $^+$ CD44 $^{\rm hi}$ T cells (activated effector T cells) in the lung tissues. (F-H) Flow cytometry plots and quantitative data represent the percentage and total numbers of CD44 $^{\rm hi}$ CD62L $^{\rm lo}$ T cells (effector memory T cells) within the CD4 $^+$ population of the brain tissues. (I-K) Flow cytometry plots and quantitative data represent the percentage and total numbers of CD44 $^{\rm hi}$ CD62L $^{\rm lo}$ T cells within the CD8 $^+$ population of brains. Results were expressed as the mean \pm S.D (n = 5 per group). *p < 0.05 versus the control group, *p < 0.05 versus the C57BL/6 group (two-way ANOVA, Bonferroni post hoc test). CD28 $^+$ C CD28 knockout mice

stops breathing after the explosion, thus indirectly affecting the functions of the heart, lung and brain (Miyazaki et al., 2015). In this study, after chest blast exposure, the serum inflammatory factors IL-4, IL-6 and HMGB1 were increased, the CD3+ T cells, CD4+ and CD8+T cell subsets in the lung tissues were activated. The percentage and total number of CD3+ T cells in the lung tissues of C57BL/6 male mice were the highest at 12 h and the lowest at 48 h. Therefore, to ensure the validity of the data, the percentage and total number of CD3+ T cells in the lung tissues of CD28-/- male mice at 24 h were selected. Moreover, chest blast exposure caused damage to the spatial learning and memory ability, BBB destruction and brain injury. Whereas CD28 KO significantly inhibited inflammatory cell infiltration and activation of CD3⁺ T cells and CD4⁺ and CD8⁺ subsets of T cells in the lung tissues, improved spatial learning and memory ability, BBB destruction and brain injury. Furthermore, CD28 KO inhibited chest blast exposure-induced increases of p-PI3K, p-AKT and NF-κB in the brain. Our data demonstrated that chest blast exposure could cause bTBI, whereas CD28 KO attenuated bTBI through the PI3K/AKT/NF-κB signaling pathway. These results provide a new target for the prevention and treatment of bTBI in veterans.

Hyperphosphorylated tau aggregates were common in neurodegenerative diseases, such as alzheimer's disease (AD), and cause cognitive dysfunction (Kametani, Hasegawa, 2018), while the bTBI was also

associated with Tau (Gyoneva et al., 2015). Choline acetyltransferase transfers acetyl-CoA to choline, leading to the formation of the neurotransmitter acetylcholine, which was involved in the regulation of the correlation between the hippocampus, hippocampal formation, and memory span and may be observed in AD (Mellott et al., 2017). The S100β was a marker of brain injury and its expression was closely related to the severity of brain injury. The moderate amount of \$100\beta protected the brain, but high levels of expression caused cerebrovascular diseases (Harpaz et al., 2021). Studies have shown that p-Tau and its combination with p-Tau/t-Tau can effectively evaluate the prognosis and mortality of bTBI patients (Wang et al., 2018). Tau protein is a member of microtubule-related proteins in nerve cells, and it will be phosphorylated to p-tau during tTBI (Wang et al., 2018). Our results indicated that chest blast exposure caused damage to the spatial learning and memory ability, BBB destruction and brain damage, increased the expression of Tau, p-Tau, S100β, and choline acetyltransferase. In the case of head protection, chest blast exposure will propagate to the head along with the blood vessels and cause brain damage (Bhattacharjee, 2008). In this study, our data showed that BBB damage peaked at 12 h, recovered at 24 h, and was aggravated again at 48 h during bTBI. As reported by Hue (Hue et al., 2016) et al., the opening of the BBB caused by the shock wave was temporary, starting from 6 h, reaching the peak opening at

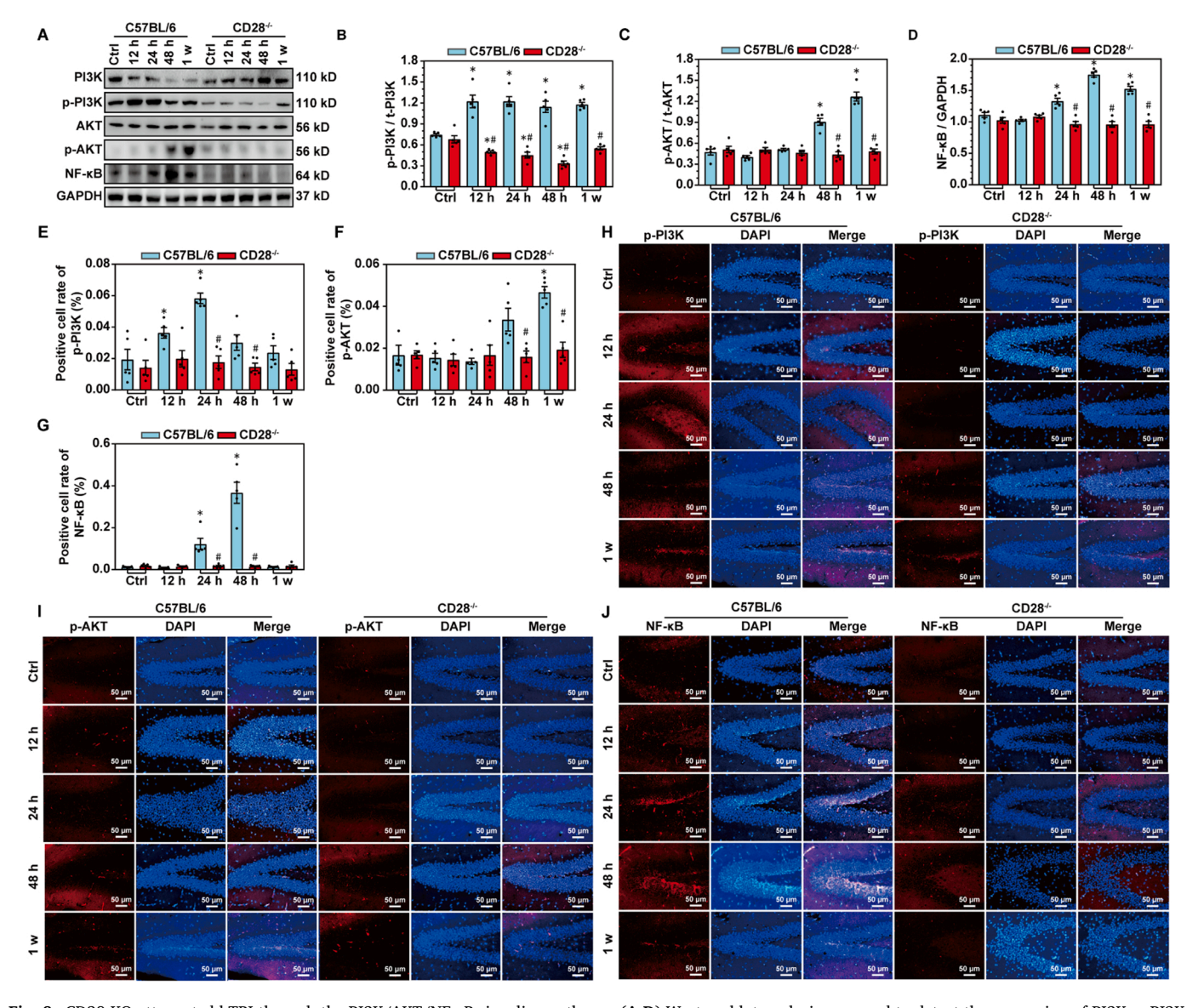


Fig. 8. CD28 KO attenuated bTBI through the PI3K/AKT/NF-κB signaling pathway. (A-D) Western blot analysis was used to detect the expression of PI3K, p-PI3K, AKT, p-AKT, and NF-κB in the brain tissues. GAPDH was used as a reference. (E-J) Immunofluorescence staining of p-PI3K, p-AKT, NF-κB (red), and DAPI (blue) was performed. The positive cell rate of p-PI3K, p-AKT, and NF-κB was analyzed. Results are expressed as the mean \pm S.D (n = 5 per group). *p < 0.05 versus the control group, *p < 0.05 versus the C57BL/6 group (two-way ANOVA, Bonferroni post hoc test). CD28 '/: CD28 knockout mice

 $12\,h,$ recovering at $24\,h,$ and opening again at $48\,h.$ Our results suggested that the TBI caused by blast exposure directly to the brain, BBB damage caused by chest blast exposure was induced by other factors besides the blast wave propagating from the delayed vessels to the brain. However, the re-opening of the BBB at $48\,h$ may be due to inflammation in the lung tissues.

Alveolar inflammation, neutrophil recruitment and cytokine production after traumatic stress, and then lung injury may increase the sensitivity of the brain to acute injury. Cytokine activated endothelial cells secrete chemokine adhesion molecules on their surface, resulting in the migration of activated immune cells across the endothelium. We speculated that this phenomenon was caused by inflammation related factors in the blood circulation. This local inflammation can spread to the systemic circulation. Pulmonary inflammation can spread to the brain system through humoral, cellular and neural pathways. The BBB destruction caused by the action of pro-inflammatory cytokines is a hallmark of cerebrovascular disorders, and then destruction of BBB might lead to neuroinflammation (Oikawa et al., 2019;Wu et al., 2019). Kaempferol alleviated LPS-induced neuroinflammation and BBB

dysfunction through inhibiting HMGB1 release and down-regulating the TLR4/MyD88 pathway (Cheng et al., 2018). Therefore, the lung injury caused by blast waves led to an increase in inflammatory factors, which then caused brain microvascular endothelial cell disorders and BBB damage. The BBB protected the brain by restricting blood-derived products, pathogens, and cells from entering the brain, maintaining normal neuronal function and information processing, whereas damage to BBB integrity induces damage to hippocampal neurons, which in turn led to cognitive impairment (Montagne et al., 2015). In summary, the BBB damage caused by chest to blast exposure is not only related to blast waves transmitted along blood vessels to the brain, but also closely related to inflammation factors released by the lung tissues.

Furthermore, the results demonstrated that CD28 KO significantly inhibited lung and brain inflammatory cell infiltration and activation of CD3⁺ T cells and CD4⁺ and CD8⁺ subsets of T cells, improved spatial learning and memory ability, reduced the BBB destruction, hippocampal neuronal damage during bTBI. The activation of T cells was positively correlated with the IL-4 content of the cell supernatant and negatively correlated with the level of serum interferon gamma (Shi et al., 2017).

The CD28 observably increased IL-6 and IL-8 expression in relapsing remitting multiple sclerosis and selectively induced IL-17A expression by stimulating IL-6-mediated signaling (Camperio et al., 2014). These studies suggested that CD28 KO could effectively inhibit the production of the inflammatory response, thereby reducing the inflammatory related factors in blood circulation. Moreover, CD3/CD28 or PMA/IROO activated the release of TNF α , which promoted CD8 $^+$ T cells and induced plasticity in the brain (Zarif et al., 2017). The CD28 inhibition also reduced cerebral hemorrhage-induced inflammatory response (Zhou et al., 2017). In addition, the CD28 super-agonist monoclonal antibody (CD28SA) promoted the CD28 and increased cerebral infarct size caused by cerebral hemorrhage, increased regulatory T cells, and enhanced the inflammatory response (Janakiram et al., 2017). These data demonstrated that the CD28 KO ameliorated brain damage caused by chest exposure to blast waves by inhibiting inflammatory cell infiltration and T-cell activation in the lung tissues.

It has been reported that CD28 signal transduction in T cells is closely related to the phosphatidylinositol 3 kinase (PI3K)/protein kinase B (AKT) pathway (Friend et al., 2006). PI3K, a direct upstream activator of AKT, plays an important role in many cell signaling pathways, cell cycle progression and cell growth (Way et al., 2016). The binding of CD28 and CD80/CD86 induced T cell activation and then activated the PI3K/AKT pathway, while downstream, phosphorylated AKT activated the NF-κB pathway to induce IL-6 expression and further enhance T cell activation (Koorella et al., 2014). Therefore, the activation of NF-κB signaling in this study is partially dependent on its upstream PI3K/Akt signaling pathway. PI3K delta, an inhibitor of AKT, could selectively stimulate the production of T-cell factors against CD3/CD28 and reduce inflammation in vivo (Way et al., 2016). Furthermore, the PI3K/AKT signaling pathway was necessary for CD28 to induce NF-κB activation (Skanland et al., 2014; Kunkl et al., 2019). Studies have shown that brain injury can also initiate neuroinflammation through the activation of PI3K/Akt and NF-κB pathways, leading to the elevation of inflammatory factors (Zhang et al., 2022). In this study, chest blast exposure leads to acute lung injury and inflammatory cell infiltration, activates peripheral blood T cells and promotes the expression and release of inflammatory factors such as IL-4, IL-6, and HMGB1. Activated T cells and inflammation factors reach the brain through blood circulation, cause BBB destruction and aggravates brain injury. In the hours to days after the initial injury, secondary damage mediated by inflammatory response is the main pathological feature of brain injury (Wang et al., 2020). Therefore, there is a certain time difference between brain injury and lung injury during the detonation event. Activation of NF-κB induces nuclear transcription and the expression of inflammatory factors, and increases the expression of Tau, p-Tau and Choline acetyl transferase, and finally caused bTBI. Therefore, these data suggested that CD28 KO ameliorated brain damage caused by chest blast exposure partly through the PI3K/AKT/NF-κB signaling pathway.

5. Conclusion

In summary, knockdown of the CD28 could reduce the expression of inflammation by down regulating PI3K/AKT/NF-κB pathways, thus playing a role in protecting brain injury. The CD28 KO targeting PI3K/AKT/NF-κB may have unique pharmacological potential in brain injury and is expected to be developed as an inflammatory attenuator. This paper provides a new idea for studying the mechanism and treatment of chest blast exposure-induced traumatic brain injury.

Funding

This work was supported by the General project of Liaoning Provincial Department of Education (LJKZ1153) and Shenyang Science and Technology Plan Project (22-315-6-17).

CRediT authorship contribution statement

Zhonghua Luo: Software, Resources, Methodology, Formal analysis, Data curation. Yunen Liu: Writing – review & editing, Resources, Investigation, Funding acquisition. Peifang Cong: Methodology, Data curation. Changci Tong: Software, Methodology, Formal analysis. Shun Mao: Methodology, Data curation. Mingxiao Hou: Writing – review & editing, Supervision. Ying Xu: Software, Methodology.

Declaration of Competing Interest

The authors declare that they have no known competing financial interests or personal relationships that could have appeared to influence the work reported in this paper.

Data Availability

The authors do not have permission to share data.

Appendix A. Supporting information

Supplementary data associated with this article can be found in the online version at doi:10.1016/j.brainresbull.2024.110987.

References

- Beamer, M., Tummala, S.R., Gullotti, D., Kopil, C., Gorka, S., Ted, A., et al., 2016. Primary blast injury causes cognitive impairments and hippocampal circuit alterations. Exp. Neurol. 283, 16–28.
- Bhattacharjee, Y., 2008. Neuroscience. Shell shock revisited: solving the puzzle of blast trauma. Science 319, 406–408.
- Camperio, C., Muscolini, M., Volpe, E., et al., 2014. CD28 ligation in the absence of TCR stimulation up-regulates IL-17A and pro-inflammatory cytokines in relapsingremitting multiple sclerosis T lymphocytes. Immunol. Lett. 158, 134–142.
- Cernak, I., 2010. The importance of systemic response in the pathobiology of blast-induced neurotrauma. Front Neurol. 1, 151.
- Cheng, X., Yang, Y.L., Yang, H., Wang, Y.H., Du, G.H., 2018. Kaempferol alleviates LPS-induced neuroinflammation and BBB dysfunction in mice via inhibiting HMGB1 release and down-regulating TLR4/MyD88 pathway. Int. Immunopharmacol. 56, 20-25.
- Dixon, K.J., 2017. Pathophysiology of Traumatic Brain Injury. Phys. Med Rehabil. Clin. N. Am. 28, 215–225.
- Evans, L.P., Roghair, A.M., Gilkes, N.J., Bassuk, A.G., 2021. Visual Outcomes in Experimental Rodent Models of Blast-Mediated Traumatic Brain Injury. Front Mol. Neurosci. 14, 659576.
- Friend, L.D., Shah, D.D., Deppong, C., et al., 2006. A dose-dependent requirement for the proline motif of CD28 in cellular and humoral immunity revealed by a targeted knockin mutant. J. Exp. Med. 203, 2121–2133.
- Gyoneva, S., Kim, D., Katsumoto, A., Kokiko-Cochran, O.N., 2015. Lamb BT and Ransohoff RM. Ccr2 deletion dissociates cavity size and tau pathology after mild traumatic brain injury. J. Neuroinflamm. 12, 228.
- Haanstra, K.G., Dijkman, K., Bashi, r N., et al., 2015. Selective blockade of CD28-mediated T cell costimulation protects rhesus monkeys against acute fatal experimental autoimmune encephalomyelitis. J. Immunol. 194, 1454–1466.
- Harpaz, D., Bajpai, R., Ng, G.J.L., et al., 2021. Blood biomarkers to detect new-onset atrial fibrillation and cardioembolism in ischemic stroke patients. Heart Rhythm 18, 855–861.
- Heldt, S.A., Elberger, A.J., Deng, Y., Guley, N.H., Del Mar, N., Rogers, J., et al., 2014. A novel closed-head model of mild traumatic brain injury caused by primary overpressure blast to the cranium produces sustained emotional deficits in mice. Front Neurol. 5, 2.
- Hue, C.D., Cho, F.S., Cao, S., et al., 2016. Time course and size of blood-brain barrier opening in a mouse model of blast-induced traumatic brain injury. J. Neurotrauma 33, 1202–1211.
- Janakiram, M., Shah, U.A., Liu, W., Zhao, A., Schoenberg, M.P., Zang, X., 2017. The third group of the B7-CD28 immune checkpoint family: HHLA2, TMIGD2, B7x, and B7-H3. Immunol. Rev. 276, 26–39.
- Kametani, F., Hasegawa, M., 2018. Reconsideration of amyloid hypothesis and Tau hypothesis in Alzheimer's disease. Front. Neurosci. 12, 25
- Konan, L.M., Song, H., Pentecost, G., et al., 2019. Multi-FOCAL NEURONAL
 ULTRASTRUCTURAL ABNORMALITIES AND SYNAPTIC ALTERATIONS IN MICE
 AFTER LOW-INTENSITY BLAST EXPosure. J. Neurotrauma 36, 2117–2128.
- Koorella, C., Nair, J.R., Murray, M.E., Carlson, L.M., Watkins, S.K., Lee, K.P., 2014. Novel regulation of CD80/CD86-induced phosphatidylinositol 3-kinase signaling by NOTCH1 protein in interleukin-6 and indoleamine 2,3-dioxygenase production by dendritic cells. J. Biol. Chem. 289, 7747–7762.
- Kunkl, M., Mastrogiovanni, M., Porciello, N., et al., 2019. CD28 individual signaling upregulates human IL-17A expression by promoting the recruitment of RelA/NF-

- kappaB and STAT3 transcription factors on the proximal promoter. Front. Immunol. 10.864.
- Langenhorst, D., Tabares, P., Gulde, T., et al., 2017. Self-recognition sensitizes mouse and human regulatory T cells to low-dose CD28 superagonist stimulation. Front. Immunol. 8, 1985.
- Langenhorst, D., Haack, S., Gob, S., et al., 2018. CD28 costimulation of T helper 1 cells enhances cytokine release in vivo. Front. Immunol. 9, 1060.
- Liu, M., Zhang, C., Liu, W., Luo, P., Zhang, L., Wang, Y., et al., 2015. A novel rat model of blast-induced traumatic brain injury simulating different damage degree: implications for morphological, neurological, and biomarker changes. Front. Cell Neurosci. 9, 168.
- Logsdon, A.F., Meabon, J.S., Cline, M.M., et al., 2018. Blast exposure elicits blood-brain barrier disruption and repair mediated by tight junction integrity and nitric oxide dependent processes. Sci. Rep. 8, 11344.
- Ma, L., Shen, X., Gao, Y., et al., 2016. Blocking B7-1/CD28 pathway diminished long-range brain damage by regulating the immune and inflammatory responses in a mouse model of intracerebral hemorrhage. Neurochem. Res. 41, 1673–1683.
- Ma, Y., Xia, X., Cheng, J.M., Kuang, Y.Q., Yang, T., Yang, L.B., et al., 2014. Emodin inhibits inducible nitric oxide synthase in a rat model of craniocerebral explosive injury. Neurochem. Res. 39, 1809–1816.
- Marsh, J.L., Bentil, S.A., 2021. Cerebrospinal fluid cavitation as a mechanism of blast-induced traumatic brain injury: a review of current debates, methods, and findings. Front Neurol. 12, 626393.
- Mellott, T.J., Huleatt, O.M., Shade, B.N., et al., 2017. Perinatal choline supplementation reduces amyloidosis and increases choline acetyltransferase expression in the hippocampus of the APPswePS1dE9 Alzheimer's disease model mice. PloS One 12, e0170450.
- Miyazaki, H., Miyawaki, H., Satoh, Y., Saiki, T., Kawauchi, S., Sato, S., Saitoh, D., 2015. Thoracic shock wave injury causes behavioral abnormalities in mice. Acta Neurochir. (Wien.) 157, 2111–2120.
- Montagne, A., Barnes, S.R., Sweeney, M.D., et al., 2015. Blood-brain barrier breakdown in the aging human hippocampus. Neuron 85, 296–302.
- Oikawa, S., Kai, Y., Mano, A., et al., 2019. Potentiating a non-neuronal cardiac cholinergic system reinforces the functional integrity of the blood brain barrier associated with systemic anti-inflammatory responses. Brain Behav. Immun. 81, 122-137.
- Ptackova, P., Musil, J., Stach, M., et al., 2018. A new approach to CAR T-cell gene engineering and cultivation using piggyBac transposon in the presence of IL-4, IL-7 and IL-21. Cytotherapy.
- Raza, Z., Hussain, S.F., Ftouni, S., et al., 2021. Dementia in military and veteran populations: a review of risk factors-traumatic brain injury, post-traumatic stress disorder, deployment, and sleep. Mil. Med. Res. 8, 55.
- Robinson, C.P., 2021. Moderate and severe traumatic brain injury. Contin. (Minneap. Minn.) 27, 1278–1300.

- Rubovitch, V., Ten-Bosch, M., Zohar, O., Harrison, C.R., Tempel-Brami, C., Stein, E., et al., 2011. A mouse model of blast-induced mild traumatic brain injury. Exp. Neurol. 232, 280–289.
- Shi, C., Xu, X., Yu, X., et al., 2017. CD3/CD28 dynabeads induce expression of the antigen in human t cells accompanied by hypermethylation of the cosmc promoter. Mol. Immunol. 90, 98–105.
- Skanland, S.S., Moltu, K., Berge, T., Aandahl, E.M., Tasken, K., 2014. T-cell costimulation through the CD2 and CD28 co-receptors induces distinct signalling responses. Biochem. J. 460, 399–410.
- Tong, C., Liu, Y., Zhang, Y., et al., 2018. Shock waves increase pulmonary vascular leakage, inflammation, oxidative stress, and apoptosis in a mouse model. Exp. Biol. Med. 243, 934–944.
- Tong, C., Cong, P., Liu, Y., et al., 2021. Tandem mass tag-based quantitative proteomic analysis reveals pathways involved in brain injury induced by chest exposure to shock waves. Front. Mol. Neurosci. 14, 688050.
- Uzunalli, G., Herr, S., Dieterly, A.M., Shi, R., Lyle, L.T., 2021. Structural disruption of the blood-brain barrier in repetitive primary blast injury. Fluids Barriers CNS 18, 2.
- Wang, H., Zhou, X.M., Wu, L.Y., et al., 2020. Aucubin alleviates oxidative stress and inflammation via Nrf2-mediated signaling activity in experimental traumatic brain injury. J. Neuroinflamm. 17 (1), 188.
- Wang, K.K., Yang, Z., Zhu, T., et al., 2018. An update on diagnostic and prognostic biomarkers for traumatic brain injury. Expert Rev. Mol. Diagn. 18, 165–180.
- Way, E.E., Trevejo-Nunez, G., Kane, L.P., et al., 2016. Dose-dependent suppression of cytokine production from T cells by a novel phosphoinositide 3-kinase delta inhibitor. Sci. Rep. 6, 30384.
- Wu, K.C., Lee, C.Y., Chou, F.Y., Chern, Y., Lin, C.J., 2019. Deletion of equilibrative nucleoside transporter-2 protects against lipopolysaccharide-induced neuroinflammation and blood-brain barrier dysfunction in mice. Brain Behav. Immun.
- Zarif, H., Nicolas, S., Guyot, M., et al., 2017. CD8(+) T cells are essential for the effects of enriched environment on hippocampus-dependent behavior, hippocampal neurogenesis and synaptic plasticity. Brain Behav. Immun.
- Zhang, T.M., Dong, Z.H., Liu, F.X., et al., 2022. Avermectin induces carp neurotoxicity by mediating blood-brain barrier dysfunction, oxidative stress, inflammation, and apoptosis through PI3K/Akt and NF-κB pathways. Ecotoxicol. Environ. Saf. 243, 113961.
- Zhou, K., Zhong, Q., Wang, Y.C., et al., 2017. Regulatory T cells ameliorate intracerebral hemorrhage-induced inflammatory injury by modulating microglia/macrophage polarization through the IL-10/GSK3beta/PTEN axis. J. Cereb. Blood Flow. Metab.: Off. J. Int. Soc. Cereb. Blood Flow. Metab. 37, 967–979.
- Zumerle, S., Molon, B., Viola, A., 2017. Membrane rafts in T cell activation: a spotlight on CD28 costimulation. Front. Immunol. 8, 1467.